

Temperature dependence of excitonic energy in isolated Se chains formed in the channels of AlPO₄-5 crystals

Sun, Handong; Tang, Z. K.; Zhao, W. M.; Wong, G. K.

1997

Sun, H. D., Tang, Z. K., Zhao, W. M., & Wong, G. K. (1997). Temperature dependence of excitonic energy in isolated Se chains formed in the channels of AlPO₄-5 crystal. *Applied Physics Letters*, 71(17), 2457-2459.

<https://hdl.handle.net/10356/101397>

<https://doi.org/10.1063/1.120113>;

<https://doi.org/10.1063/1.120113>

Applied Physics Letters © copyright 1997 American Institute of Physics. The journal's website is located at <http://apl.aip.org/>.

Downloaded on 04 Apr 2024 17:56:54 SGT

Temperature dependence of excitonic energy in isolated Se chains formed in channels of $\text{AlPO}_4\text{-5}$ crystals

H. D. Sun,^{a)} Z. K. Tang, W. M. Zhao, and George K. L. Wong

Physics Department, Hong Kong University of Science and Technology, Clear Water Bay, Kowloon, Hong Kong

(Received 8 July 1997; accepted for publication 26 August 1997)

Optical absorption spectra of Se chains formed in channels of $\text{AlPO}_4\text{-5}$ (AFI) crystals are measured in the temperature range from 80 to 298 K. The excitonic energy of the isolated Se chains is observed to shift to lower energy linearly with increasing temperatures, in sharp contrast to the positive temperature coefficient in trigonal-Se crystal. The marked change in the temperature behavior of the excitonic energy is attributed to the greatly diminished interchain interaction in Se-AFI as well as the weakening of the electron-optical-phonon coupling in a low-dimensional system. © 1997 American Institute of Physics. [S0003-6951(97)01643-4]

Bulk solids consist of atoms or molecules, yet the properties of solids can be totally different from their constituent atoms or molecules. Nanometer-size structures provide an opportunity to observe and control the properties of materials as they evolve from atoms or molecules to the bulk. In nanostructured semiconductors, carriers are confined spatially and occupy quantized discrete energy levels. This makes nanostructured materials possess novel properties, such as large optical nonlinearity, ultra-high-speed optical response, superparamagnetism,¹⁻⁴ etc. The confinement induced blue-shift of the excitonic energy with decreasing crystal size is well established. Experimentally, however, the discrete nature of these states is usually concealed by sample inhomogeneities such as distributions in size and shape. Zeolites provide us with ideal templates for assembling monodispersed nanometer-size structures because they contain uniform-sized pores (channel or cage), which have the ability to absorb molecular species.^{3,5-8} For example, zeolite Linder-type A has cages with a diameter of 11 Å, which are connected to each other in a simple cubic structure by sharing windows of 4 Å in diameter.⁹ Zeolite $\text{AlPO}_4\text{-5}$ has open channels that are parallelly packed in a hexagonal structure.¹⁰ The inner diameter of the channel is 7.3 Å, and the distance between two neighboring channels is 13.7 Å.

Trigonal-Se crystal (*t*-Se) is known to consist of parallel packed helical chains, as shown in Fig. 1. The intrachain charge transfer interaction dominates the atom-atom interactions, which gives rise to its strong chain characteristics. The electronic configuration of the Se atom is $4s^24p^4$. Two $4p$ electrons contribute to the covalent bond (σ) between neighboring Se atoms and form a helical chain structure. The remaining two $4p$ electrons are in lone-pair (LP) states that form the uppermost valence band, while the empty $4p$ antibonding states (σ^*) form the lowest conduction band. There is an energy gap between the LP and σ^* bands.¹¹⁻¹³ Both direct and indirect optical transitions between LP and σ^* show abnormal temperature behavior: below 100 K the band-gap energies increase with increasing temperatures due to the lattice dilation determined by acoustic phonons. Above 100 K, the electron-optical-phonon interaction is increas-

ingly of importance, leading to a bending of the temperature shift of the band-gap energies.¹⁴ According to the band-structure calculation of Ikawa,¹² an ideal single Se chain is of a similar electronic structure to that of *t*-Se crystal. However, very few experimental works have been reported on optical properties of isolated Se chains.^{5,11,15,16}

In this letter, the temperature dependence of optical absorption spectra are reported for Se chains isolated in the channels of $\text{AlPO}_4\text{-5}$ crystals. Hereafter, $\text{AlPO}_4\text{-5}$ is termed as AFI as recommended by IUPAC. The temperature dependence of the excitonic energy of isolated Se chains is found to be considerably different from that of *t*-Se crystal, though the helical symmetry and electronic structure of the isolated Se chains are very similar to those of *t*-Se. We show that the different temperature behaviors of the excitonic energy can be attributed to the diminished interchain interaction in Se-AFI and the weakening of the electron-optical-phonon coupling in the low-dimensional system.

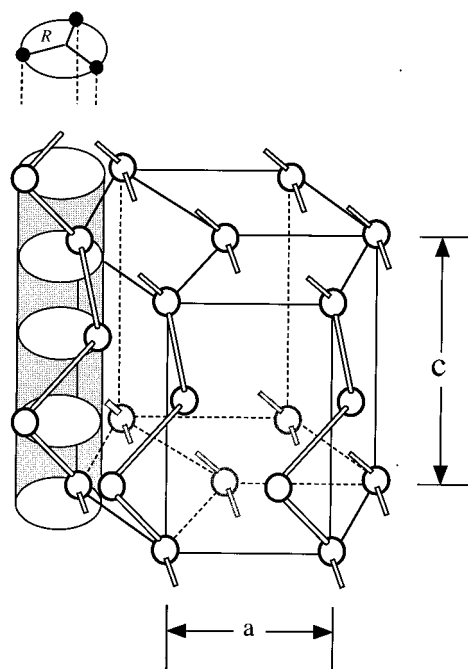


FIG. 1. The crystal structure of trigonal selenium.

^{a)}Electronic mail: phsunh@usthk.ust.hk

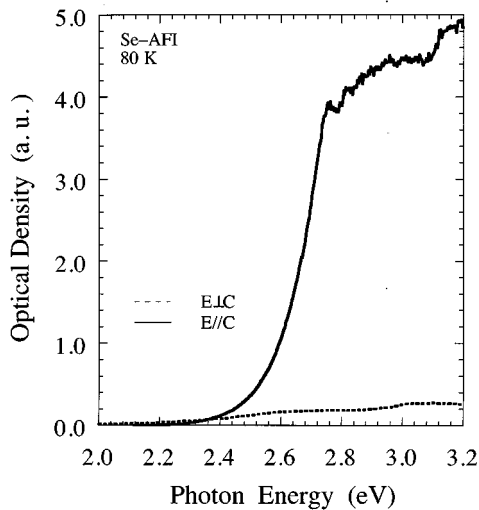


FIG. 2. The absorption spectra at 80 K of Se chains isolated in the channels of AFI for light polarized parallel to the crystal axis c ($E\parallel c$) and perpendicular to c ($E\perp c$).

We use AFI single crystals with dimensions of about 0.5 mm in length and 30 μm in cross section diameter to form Se chains. Refined pure Se was introduced into the channels of AFI crystals by physical adsorption through vapor phase diffusion at about 250 $^{\circ}\text{C}$. The details of sample preparation were described in Ref. 17. As-prepared Se-AFI is light yellow in color while the original AFI crystal is transparent. Polarized microscopy showed that selenium atoms are distributed uniformly in the channels. Polarized micro-Raman scattering experiments showed that the atoms of Se chains isolated in the channels are arranged in helical structure with D_3 symmetry.¹¹ Transmission spectra were measured at different temperatures, using a tungsten-halogen incandescent lamp as a light source. The incident light was dispersed by a 275 mm monochromator and focused onto a sample using a reflecting microscope objective. The transmitted light was collected using another identical reflecting objective and coupled to an optical fiber. The optical signal was detected using a photomultiplier and processed by a lock-in amplifier. The sample was mounted on a specially designed stage, the temperature of which can be controlled from 77 K to room temperature. Because of the small size of the zeolite crystals, care was taken in mounting the sample to ensure that it attains the temperature of the sample stage and the samples do not move during cooling and heating.

Figure 2 shows the absorption spectra at 80 K of Se chains formed in the channels of AFI for light polarized parallel to the crystal axis c ($E\parallel c$) and perpendicular to c ($E\perp c$). The sample behaves as a good polarizer with high absorption for the $E\parallel c$ polarization and with high transparency for the $E\perp c$ polarization. An undoped AFI crystal is highly transparent for both polarization directions. The lowest absorption band for the Se-AFI is located at about 2.6 eV in the $E\parallel c$ polarization, which is blueshifted by about 0.6 eV from the direct-gap excitonic transition of t -Se crystal.¹⁷

Figure 3 shows the optical absorption spectra at several temperatures ranging from 80 to 298 K. The lowest absorption band shifts to lower energy with increasing temperatures. In Fig. 4, the energy position of the lowest absorption

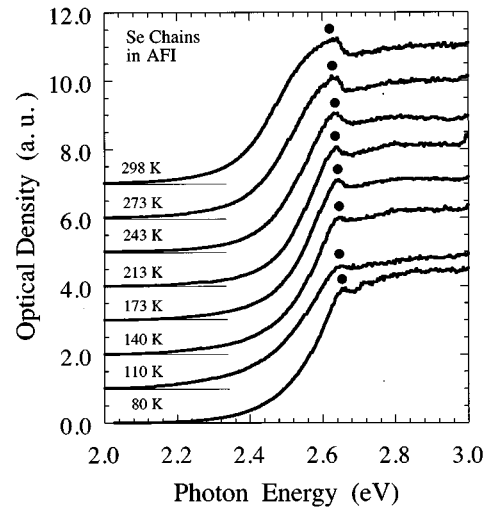


FIG. 3. The optical absorption spectra at different temperatures ranging from 80 to 298 K.

band is plotted as a function of temperature. The temperature dependence of the indirect (open circles) and the first direct (solid circles) excitonic energies of t -Se (Ref. 14) are also shown in Fig. 4. The excitonic energy of Se-AFI decreases linearly as a function of increasing temperature, which is in sharp contrast to the temperature dependence of the excitonic energy of t -Se, which has a positive temperature coefficient at the low-temperature region and with a bended temperature shift near room temperature.

Because of the strong chain character of t -Se crystal, the electronic structure of an isolated Se chain is not expected to differ much from that of t -Se crystal, although the lattice parameters (bond length r , bond angle θ , and dihedral angle Ψ) of an isolated chain are slightly different from those of t -Se.¹¹ The small blueshift of the lowest excitation energy of Se-AFI indicates that the isolation of Se chains has a weak effect on the electronic structure. However, the lowest exci-

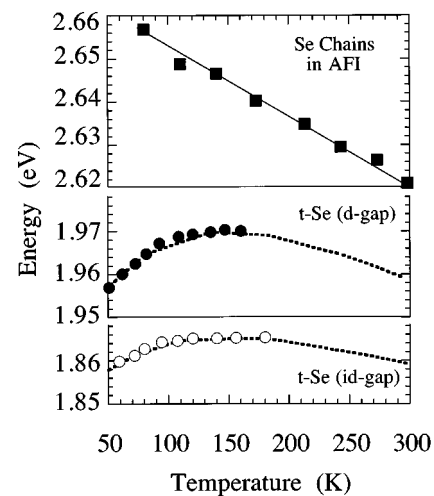


FIG. 4. The excitonic energy of indirect gap (open circles) and direct gap (solid circles) of t -Se crystal, and that of the isolated Se chain in AFI channels (square dots) plotted as a function of temperature. The data of t -Se crystal is quoted from Ref. 14. The dashed curves are the theoretical fits by considering the contribution of both lattice dilation and electron-optical-phonon coupling for t -Se crystal. The solid line is the linear fit of the experimental data for Se-AFI.

tonic energy has a completely different temperature dependence for the isolated chain than that for *t*-Se crystal, as shown in Fig. 4. This difference can be understood by considering the lattice dilation and electron-optical-phonon coupling contributions to the excitonic energy. At temperature *T*, the gap energy of *t*-Se can be written as

$$E_g(T) = E_0 + E_p(T) + E_D(T), \quad (1)$$

where E_0 is the gap energy at zero temperature, E_p is the contribution of electron-optical-phonon coupling in the absence of any distortion of the lattice, which leads to a decrease of the gap energy with increasing temperatures,¹⁴ and E_D is the contribution of the lattice dilation. For *t*-Se crystal, the thermal dilation induced band-gap energy shift has three contributions that can be written as¹⁴

$$\left(\frac{\partial E}{\partial T}\right)_{\text{dil}} = \Xi_a \alpha_a + \Xi_c \alpha_c + \Xi_R \alpha_R, \quad (2)$$

where α_a , α_c , and α_R are the thermal expansion coefficients of the interchain distance *a*, the unit cell length *c*, and the helical chain radius *R*, respectively, and Ξ_i ($i = a, c, R$) is the corresponding deformation potential. According to a model calculation based on a simple anharmonic approximation,¹⁸ the thermal dilation of the lattice is dominated by interchain acoustic phonons and its effect is described by the first term in Eq. (2). This term gives rise to a sizable increase of the gap energy with increasing temperatures. The contributions to the temperature shift from the second term due to thermal dilation of *c* and the third term due to the dilation of *R* are negative, while the second term is negligibly small.¹⁴ When temperature is not very high, the population of the optical phonon is small and the temperature shift of the excitonic energy is dominated by the thermal dilation. Thus, the positive temperature coefficient of the gap energy of *t*-Se mainly results from the large contribution of the thermal dilation due to interchain acoustic phonons. In the high-temperature region, the contribution of the electron-optical-phonon coupling is increased, leading to a bending effect on the temperature dependence of the band-gap energy, as shown in Fig. 4.

The helical Se chains in Se-AFI are isolated and the interchain interaction is expected to be much smaller because of the large distance (13.7 Å) between neighboring channels in AFI. This has been confirmed by the absence of the phonon mode due to interchain vibration in Raman spectra.¹¹ Hence, the thermal dilation due to the interchain acoustic phonons [the first term in Eq. (2)] would no longer contribute to the temperature shift of the excitonic energy in Se-AFI. The total temperature coefficient of excitonic energy for Se-AFI is then given by

$$\frac{dE}{dT} = \Xi_c \alpha_c + \Xi_R \alpha_R + \left(\frac{\partial E}{\partial T}\right)_p, \quad (3)$$

Where $(\partial E/\partial T)_p$ is the temperature coefficient due to the electron-optical-phonon coupling without lattice deformation.

The temperature shift of the excitonic energy due to the electron-acoustic-phonon coupling (lattice dilation) is approximately a linear function of temperature, while the tem-

perature shift due to the electron-optical-phonon coupling is nonlinear with temperature.¹⁴ The excellent linear decrease of the excitonic energy with increasing temperatures in Se-AFI shown in Fig. 4 implies that the main contribution to the temperature shift of the isolated Se chain is due to lattice dilation, and the contribution from electron-optical-phonon coupling is negligible. From the experimental data shown in Fig. 4, the temperature coefficient of the excitonic energy is calculated to be -0.19 meV/K for Se-AFI. This value is in good agreement with the value of -0.2 meV calculated from the first two terms of Eq. (3),¹⁴ which again supports the assertion that the contribution to the temperature shift of the excitonic energy is mainly due to the intrachain electron-acoustical-phonon coupling and the electron-optical-phonon coupling is negligibly small in the isolated chain system because of the weakening of the Frohlich coupling strength in low-dimensional systems.^{19,20}

In summary, the temperature dependence of optical absorption spectra of isolated Se chains stabilized in the channels of AFI crystals has been studied. The lowest absorption band of Se-AFI shifts to lower energy with increasing temperature ranging from 80 to 298 K. This temperature dependence is remarkably different from that of bulk *t*-Se crystal. In Se-AFI, the interchain interaction can be neglected, and the temperature coefficient of excitonic energy is dominated by the thermal dilation of the radius of helical chains. The electron-optical-phonon coupling in Se-AFI is not important because of the weakening of the Frohlich coupling strength in a low-dimensional system.

This work was supported by the CERG grant from the Research Grants Committee of Hong Kong.

¹ Y. Wang and N. Herron, *J. Phys. Chem.* **95**, 525 (1991).

² S. Schmott-Rink, *Phys. Rev. B* **35**, 8113 (1987).

³ *Advanced Zeolite Science and Application*, edited by J. C. Jansen, M. Stiker, H. G. Karge, and J. Weitkamp (Elsevier Science, New York, 1994), pp. 115–144.

⁴ T. Goto, Yasuo Nozue, and Tetsuya Kodaira, *Mater. Sci. Eng. B* **19**, 48 (1993).

⁵ V. N. Bogolomov, S. V. Kholodkevich, S. G. Romanov, and L. S. Agroskin, *Solid State Commun.* **3**, 181 (1983).

⁶ G. A. Ozin, *Adv. Mater.* **4**, 612 (1992).

⁷ N. Herron, *J. Inclusion Phenom.* **2**, 283 (1987).

⁸ G. D. Stucky and J. E. MacDougall, *Science* **247**, 669 (1990).

⁹ V. M. Bogomolov, *Sov. Phys. Usp.* **21**, 77 (1978).

¹⁰ J. M. Bennett, J. P. Kohen, E. M. Flanigen, J. J. Pluth, and J. V. Smith, *ACS Symp. Ser.* **218**, 109 (1983).

¹¹ Z. K. Tang, M. M. T. Loy, T. Goto, J. Chen, and R. Xu, *Solid State Commun.* **101**, 333 (1997).

¹² A. Ikawa, *J. Phys. Soc. Jpn.* **63**, 1986 (1994).

¹³ A. Ikawa, *J. Non-Cryst. Solids* **117/118**, 328 (1990).

¹⁴ W. Lingelbach and G. Weiser, *Phys. Status Solidi B* **70**, 461 (1975).

¹⁵ Y. Nozue, T. Kodaira, O. Terasaki, T. Goto, D. Watanabe, and J. M. Tomas, *J. Phys.: Condens. Matter* **2**, 5209 (1990).

¹⁶ Y. Katayama, M. Yao, Y. Ajaro, M. Inui, and H. Endo, *J. Phys. Soc. Jpn.* **58**, 1811 (1989).

¹⁷ Z. K. Tang, M. M. T. Loy, Jiesheng Chen, and Ruren Xu, *Appl. Phys. Lett.* **70**, 34 (1997).

¹⁸ G. S. Guenzer and A. Bienenstock, *Phys. Rev. B* **8**, 4655 (1973).

¹⁹ Z. K. Tang, Y. Nozue, and T. Goto, *Mater. Sci. Eng. B* **35**, 410 (1995).

²⁰ S. Schmidt-Rink, D. A. B. Miller, and D. S. Chemla, *Phys. Rev. B* **35**, 811 (1986).